FOSSEE, IIT Bombay
OpenFOAM Case Study Project
July 2024

Fluid Solid Interaction (FSI) using solids4Foam

Lucky Babu Jayswal[1] and Chandan Bose[2]

[1]Undergraduate Student, Aerospace Engineering, IOE, Pulchowk Campus, Tribhuvan University
[2]Assistant Professor, Aerospace Engineering, College of Engineering and Physical Sciences, The University of Birmingham

September 23, 2024

Synopsis

Abstract

The goal of this case study project is to dig into the complexities and methodologies involved in solving Fluid-Solid Interaction (FSI) problems using the OpenFOAM toolbox, specifically solids4 Foam. The study underscores the growing interest in FSI within the computational fluid dynamics (CFD) community due to its broad applicability across various engineering fields such as aerospace and mechanical engineering. This project emphasize the inherent challenges in FSI problems, primarily due to the dynamic mesh treatment required to accurately capture the interactions between fluids and solids. The core of the report is centered around the implementation and validation of the solids4Foam solver through two distinct case studies: the Hron-Turek benchmark and a Perpendicular Flap Case.. Hron-Turek case is very popular benchmark case used to assess the accuracy of a solver developed for solving FSI problems. The Perpendicular Flap case involves a flexible flap interacting with a laminar incompressible flow within a rectangular channel, with the fluid inlet velocity varying parabolically. Both cases serve to validate the solver's accuracy by comparing the results against existing numerical data. Solids4foam employs a partitioned approach used to solve FSI problems, in which the solid and fluid domain are calculated separately. A separate coupling algorithm is used to transfers the fluid forces and solid displacement into one another. Dirichlet boundary condition is used for solving velocity near around interface while Neumann boundary condition is used for solving traction or forces around interface. This method is crucial for ensuring stable and accurate solutions in FSI simulations.The report showcases the potential of solids4Foam as a powerful tool for solving FSI problems within the OpenFOAM framework. By addressing the key challenges and providing validated case studies, valuable insights into the capabilities and applications of this open-source solver are gained, reinforcing its utility for researchers and engineers in the field of computational mechanics.

Keywords: FSI, OpenFoam, CFD, solids4foam, HronTurek, Dirichlet, Neumann

1 Introduction

1.1 Theory

Solids4foam [1]is an openfoam toolbox used for solving fluid solid interaction (FSI) problems generally. It can also be used as solid solver only to solve solid problems. It makes use of finite volume method (FVM) instead of finite element method (FEM) to calculate stresses and displacement in solids. Solids4foam uses partioned approach to solve the fluid and solid rather than monolithic approach where solid and fluid are solved simultaneously. In partioned approach, fluid and solid domain are solved separately. Strongly Coupled Dirichlet-Neumann coupling algorithm [2] is employed in the solids4foam where dirichlet and neumann boundary condition is used for calculating velocity and traction at the interface respectively.

A FSI solver based on the finite volume method is described in the paper [3] in which a strongly coupled partioned approach is used. The very famous Navier-Stokes (NS) equation is used for solving incompressible fluid flow problems using ALE approach. The solid is solved by Saint Venant Kirchoff hyperelastic model using a lagrangian approach. Finite volume method (FVM) is used for discretization of fluid and solid domain. Time discretisation is done by implicit scheme which has accuracy of second order. Similarly, space discretisation is done by cell centered method which has also accuracy of second order. This method was implemented in openfoam which is free and open source software where the FSI problems is solved using parallel processing by decomposing the domain into multiple domains. It shows quite accurate results with benchmark cases.

Fluid-Structure Interaction (FSI) benchmarks are essential for assessing numerical methods in computational mechanics, as they combine fluid dynamics with structural mechanics to model the interaction between fluid flow and structural deformation. Building on classic benchmarks like Turek and Schäfer's study of laminar flow around a cylinder and Wall and Ramm's stabilized Arbitrary Lagrangian-Eulerian finite element method, the paper [4] introduces new benchmarks which uses incompressible flow in channel around an elastic flap like body. The benchmarks emphasize capturing the oscillations induced itself in the structure, a phenomenon sensitive to numerical accuracy and stability. Numerical methods for FSI are classified into partitioned and monolithic approaches, with significant contributions from Hron and Turek in developing monolithic solvers. The proposed benchmarks include detailed specifications of fluid and structural properties, boundary conditions, and domain geometry, making use of NS equations for fluid and linear elasticity for structure. Key quantities for comparison are the y-coordinate of the beam's end over time and fluid forces on the submerged body, providing a basis for assessing the performance of FSI solvers. Testing with different material properties, such as polybutadiene and polypropylene paired with glycerine, enhances the benchmarks' robustness.

The remaining report consists of two major parts for each case and each of them are divided into three major sections. Governing Equations and Models section, defines the problem, establishes the necessary governing equations, provides an overview of the geometry and the mesh, and details of the solver setup. Next section goes over the results. This section interprets the results of the grid convergence studies and validation of the results. The final section provides a conclusion of the study.

CASE 1: PerpendicularFlap

2 Governing Equations and Models

2.1 Problem definition

This study investigates the FSI between flexible flap and laminar incompressible flow. The geometry of the problem consists of a rectangular horizontal channel and a perpendicular flexible flap. The flap is attached at the bottom of the channel. The inlet velocity of the fluid varies parabolically with the width of the channel. Low Reynold's number flow of 25 is used in this case. Two different coupling algorithms are used for fluid-solid coupling and results obtained from them are compared with each other.

2.2 Governing equations

Fluid, solid, and the interface between them are governed by three sets of equations.

2.2.1 Fluid

Incompressible flow in the fluid domain is considered and solved using the Navier-Stokes equations whose reduced form is given as:

$$\boldsymbol{\nabla \cdot V} \;=\; 0 \tag{1}$$

$$\frac{\boldsymbol{\partial \mathbf{V}}}{\boldsymbol{\partial \mathbf{t}}} \;+\; \boldsymbol{V(\nabla \cdot V)} \;=\; \nu\, \boldsymbol{\nabla^2}\, \boldsymbol{V} \;-\; \frac{1}{\rho}\boldsymbol{\nabla} p \;+\; f_b \tag{2}$$

where,
Bold symbol represents vector.
v = velocity vector
ν = Kinematic viscosity
f_b = force vector
p = pressure
ρ = density

2.2.2 Solid

We assume finite strains, with the material behavior represented by the neo-Hookean hyperelastic model:

$$\rho \frac{\partial^2 \boldsymbol{u}}{\partial t^2} \;=\; \boldsymbol{\nabla \cdot \sigma} \;+\; \rho \boldsymbol{g} \tag{3}$$

where,

$$\boldsymbol{\sigma} \;=\; \frac{1}{J}[\frac{K}{2}(J^2 \;-1)\boldsymbol{I} \;+\; \mu\, J^{-\frac{2}{3}} dev[\boldsymbol{F \cdot F^{\mathbf{T}}}]]$$

$$\boldsymbol{F} = \boldsymbol{I} + (\boldsymbol{\nabla_0 u})^{\mathrm{T}}$$

$$\boldsymbol{J} = det[\boldsymbol{F}]$$

u = displacement vector
σ = stress

2.2.3 Fluid-Solid Interface

Near the intesection in between fluid and solid region, both forces and displacement should be valid.

Those conditions require that both dispacement as well as velocity be continuous at the interface.

$$\mathbf{v}_{\mathbf{fluid}}^{[\mathbf{i}]} = \mathbf{v}_{\mathbf{solid}}^{[\mathbf{i}]} \tag{4}$$

$$\boldsymbol{u}_{\mathbf{fluid}}^{[\mathbf{i}]} = \mathbf{u}_{\mathbf{solid}}^{[\mathbf{i}]} \tag{5}$$

The dynamic conditions, obtained from the conservation of linear momentum, says that the forces are in balance.

$$\boldsymbol{n}^{[\mathbf{i}]} \cdot \sigma_{\mathbf{fluid}}^{[\mathbf{i}]} = \mathbf{n}^{[\mathbf{i}]} \cdot \sigma_{\mathbf{solid}}{}^{[\mathbf{i}]} \tag{6}$$

2.3 Geometry and Mesh

The geometry contains a horizontal channel which is 4 m in height and 8 m in length. An elastic flap, 0.1 m wide and 1 m high, is connected to the bottom of the channel 2 m from the inlet. The flap has aspect ratio (AR) of 10. The geometry is illustrated in Figure 1.

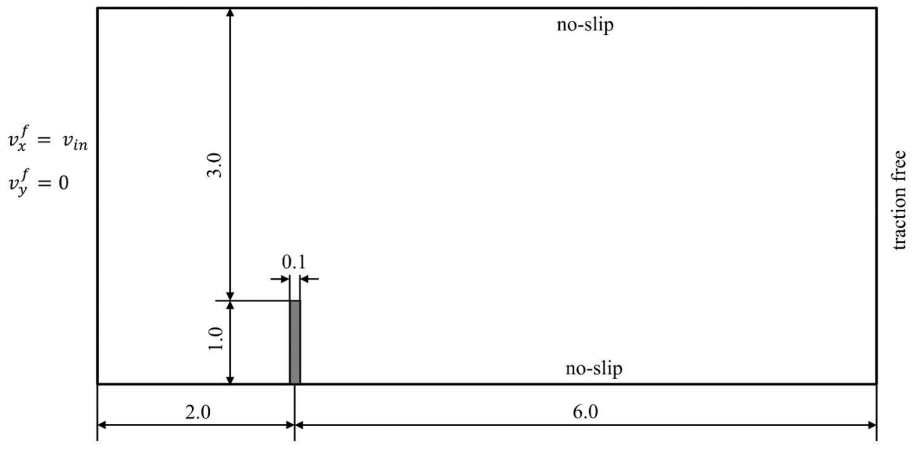

Figure 1: Computational domain and solid geometry

Meshing is done using OpenFoam BlockMesh Utility. In the FSI problem, while using the partitioned approach, the fluid domain and solid should be meshed separately since they are solved

using different equations. The fluid domain is divided into six different blocks and simple grading is used to create finer mesh near the solid as shown in Figure 2. Similarly, a solid domain is meshed considering it as a single block as shown in Figure 3. Only hexahedral cells are used during the meshing of both fluid and solid domains.

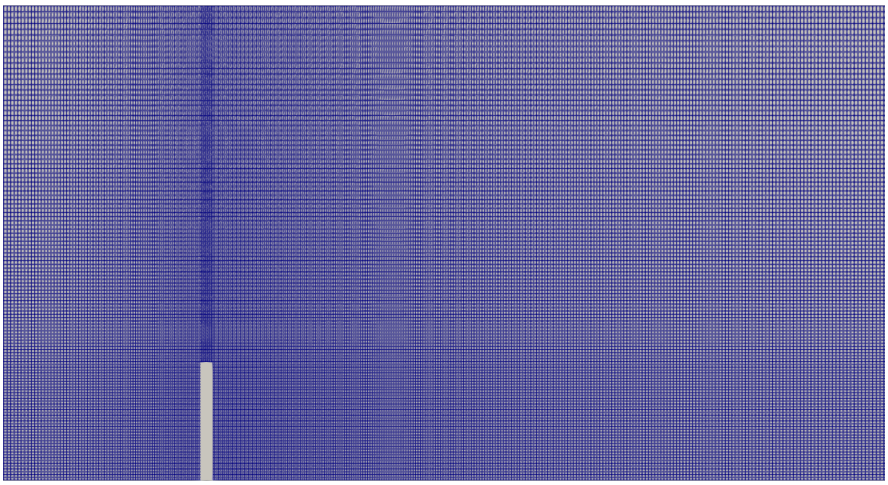

Figure 2: Mesh showing Fluid Domain

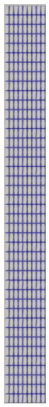

Figure 3: Mesh showing Solid

2.4 Solver setup

The solver setup can be breakdown into three different parts: Fluid Setup, Solid Setup, and Coupling Setup

2.4.1 Fluid Setup

2.4.1.1 Initial and Boundary Conditions

The velocity of fluid defined about the inlet changes parabolically along the width of the flap, as given by equation 7. The mean value of velocity (v_m) about the inlet is 1 m/s, where velocity is zero in y and z axes. The Reynolds number is associated with the velocity scale of v_m and the length scale of the flap (1 m), is fixed to be 25.

$$v^f(0,\ y)\ =\ 6v_m\frac{y}{4.0}\left(1.0-\frac{y}{4.0}\right)\ m/s \tag{7}$$

The boundary conditions applied to all patches are listed in Tables 1 and 2.

Patch	Velocity	Pressure
inlet	transitionalParabolicVelocity	zeroGradient
outlet	zeroGradient	fixedValue
flap	movingWallVelocity	zeroGradient
UpperWall	noSlip	zeroGradient
LowerWall	noSlip	zeroGradient
frontAndBack	empty	empty

Table 1: Boundary Conditions for fluid domain

Patch	Point Displacement
flap	solidTraction
bottom	fixedDisplacement
frontAndBack	empty

Table 2: Boundary Conditions for solid domain

2.4.1.2 Fluid Properties

The density of the fluid is considered to be 1 kg/m^3. Based on the Reynolds number value i.e. 25, kinematic viscosity associated with the fluid is calculated using the equation 8.

$$Re\ =\ \frac{v_m l}{\nu} \tag{8}$$

The value of kinematic viscosity is obtained to be 4e-2 m^2/s using the length scale to be 1 m and mean velocity to be 1 m/s. The flow is assumed to be in the laminar regime.

2.4.1.3 Dynamic Mesh Treatment

A mesh morphing approach is used in Solids4Foam to update the mesh regularly as the solid deflects and changes the fluid mesh. VelocityLaplacian Solver is used to handle the mesh motion within which the diffusivity quadratic inverseDistance method is selected.

2.4.1.4 Finite Volume Schemes

Operation and their Schemes are tabulated in Table 3.

Operation	Scheme
Time Derivative	Backward
Gradient	Gauss Linear

Divergence	default none;
	div(phi,U) Gauss upwind;
	div((nuEff*dev2(T(grad(U))))) Gauss linear;
	div((nuEff*dev(T(grad(U))))) Gauss linear;

Laplacian	Gauss linear corrected
Surface Normal Gradient	corrected
Interpolation	linear

Table 3: Finite Volume Schemes

2.4.1.5 Solution Method and Control

The "preconditioned Conjugate Gradient (PCG)" solver associated with a "Diagonal-based Incomplete Cholesky (DIC) preconditioner" is employed for pressure. The smoothSolver with a symGaussSeidal smoother is applied to solve velocity and cell displacement. The tolerance for pressure is fixed to 1e-8, while for velocity and cell displacement, it is fixed to 1e-6.

2.4.2 Solid Setup

2.4.2.1 Boundary Conditions

One end of the flap is attached rigidly to the bottom of the channel and the other end is set free to deflection. It acts like a cantilever beam. The flap is not allowed to deflect in the z direction. When the fluid imparts pressure and viscous force to the flap then the flap deflects and becomes steady when the flow becomes fully developed after some time.

2.4.2.2 Material Properties

The density ratio between the solid and fluid is assumed to be 10. The material properties of the flap, which represent the solid, are listed below:

- Density = 10 kg/m^3

- Youngs Modulus = 20 KPa
- Poisson Ratio = 0.3

2.4.2.3 Control

The time step of 1e−3 s is used.

2.4.3 Coupling Setup

Within the partitioned approach of two-way FSI, there can be two further different approaches: weak coupling and strong coupling. Weak coupling is also known as explicit coupling, and strong coupling is also known as implicit coupling. In implicit coupling, multiple iterations are done within a single coupling timestep to satisfy the dynamic and kinematic coupling conditions. In explicit coupling, only a single iteration is done without regard for dynamic and kinematic coupling conditions. In FSI cases like this, where the deflection is large, implicit coupling is a better approach as the accumulated error becomes too significant in explicit coupling. Two different coupling algorithms are used namely AITKEN and IQNILS. Value of 1e-6 is used as the tolerance for fluid solid interaction loop associated with each time step. And the maximum number of outer fluid solid interaction loop correctors is used as 20 associated with each time step. The relaxation factor is kept to 0.1 and the coupling is enabled from the start. DirectMap is used as the method for transferring information between the interfaces.

3 Results and Discussions

3.1 Convergence Tests

3.1.1 Grid Size Convergence Test

Three different meshes are made using blockMesh for the Grid Convergence Test. This was conducted to make sure that the results doesn't depend upon the cell size. A mesh refinement factor of two is used to create the coarse, medium, and fine mesh. This is done for the solid and fluid domains separately. The number of cells for all three coarse, medium, and fine mesh is tabulated in the Table 4 for fluid and solid separately.

Mesh	Fluid Domain	Solid
Fine	42997	378
Medium	21625	180
Coarse	10815	84

Table 4: Number of cells for different meshes

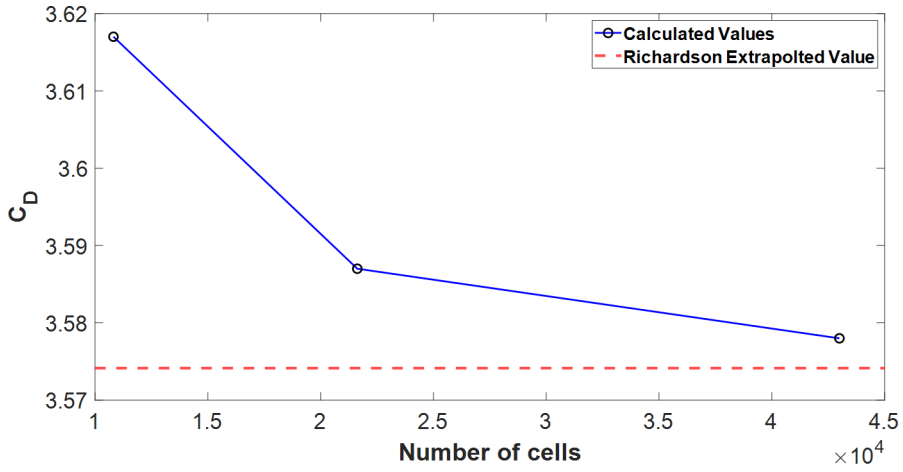

Figure 4: Grid Convergence Study

The dimensionless displacement and the drag coefficient for three different meshes are tabulated in the Table 5 and 6 using both AITKEN and IQNILS coupling algorithms. Richardson extrapolation is done using the methodology mentioned in reference [5] to obtain the drag coefficient values when the cell size tends to zero. Ideally, this means an infinite number of cells in the fluid and solid domain.

AITKEN	Displacement	Drag Coefficient (C_D)
Coarse	0.1183	3.617
Medium	0.1236	3.587
Fine	0.1264	3.578

Table 5: Values obtained using AITKEN coupling algorithm

IQNILS	Displacement	Drag Coefficient (C_D)
Coarse	0.1184	3.616
Medium	0.1244	3.603
Fine	0.1272	3.596

Table 6: Values obtained using IQNILS coupling algorithm

Then the relative percentage error is calculated for the drag coefficient values obtained for all three meshes by comparing with the Richardson extrapolated value i.e. 3.5741 for C_D which is shown in Table 7. By setting the criteria to be 0.4 % error and time for computation, the medium mesh is chosen as the best one.

Mesh	Drag Coefficient (C_D)	Relative Error (%)
Coarse	3.617	1.2
Medium	3.587	0.36
Fine	3.578	0.10

Table 7: Comparison with richardson extrapolated value

3.1.2 Time Step Convergence Test

Time step convergence test is not done due to limited computational resources.

3.2 Validation

The converged values of drag coefficient and displacement for both the AITKEN and IQNILS coupling algorithms are compared with each other. Similarly, the data obtained with solids4foam is again compared with the results obtained with different solvers. The values are within the relative error of 3 % for both AITKEN and IQNILS.

3.3 Results

The x direction displacement is normalized with the length scale of the flap and similarly, time is normalized using mean inlet velocity and length scale. The mean inlet velocity in our case is 1 m/s and the length scale is 1m. This is done for the ease of comparing data with the flap having different lengths. Dimensionless displacement versus dimensionless time is plotted and compared with the results obtained from other solvers as shown in Figure 5. Similarly, the drag coefficient is plotted against normalized time and compared with the results obtained from other solvers as shown in Figure 6.

In Figure 8, displacement contours for the flexible flap and velocity contours in the fluid domain are shown simultaneously. It shows the position of the flap when the flap attains steady deflection after the flow becomes fully developed.

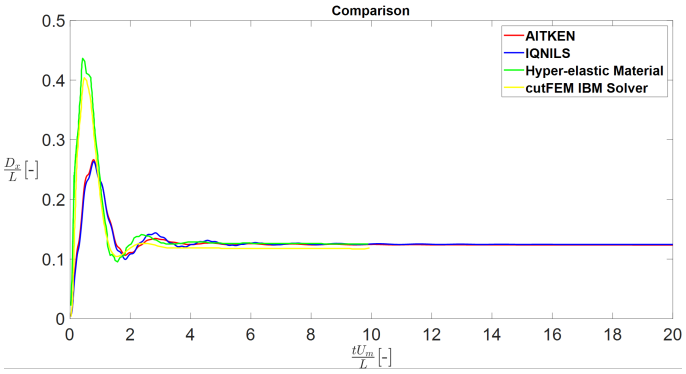

Figure 5: Displacement Comparison using different solvers

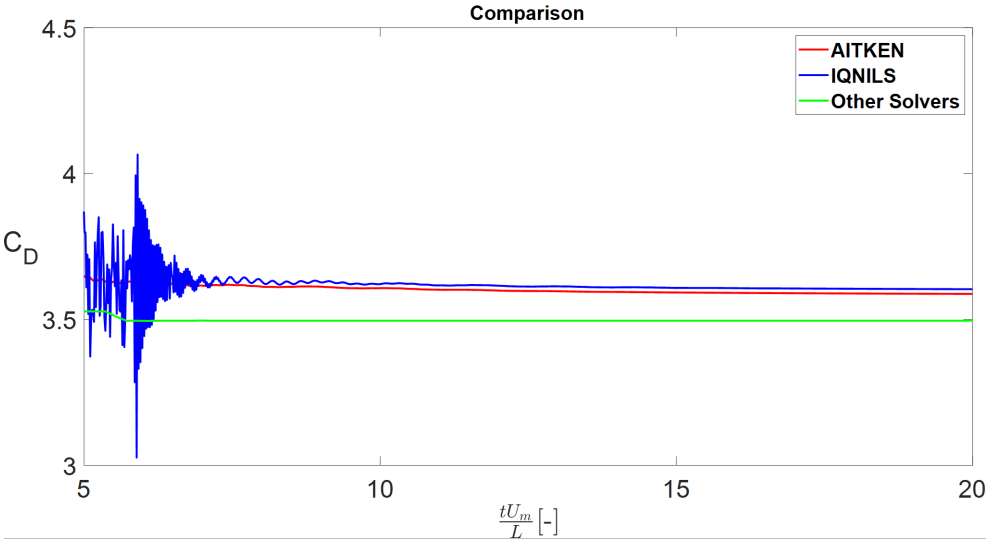

Figure 6: Drag Coefficient Comparison using different solvers

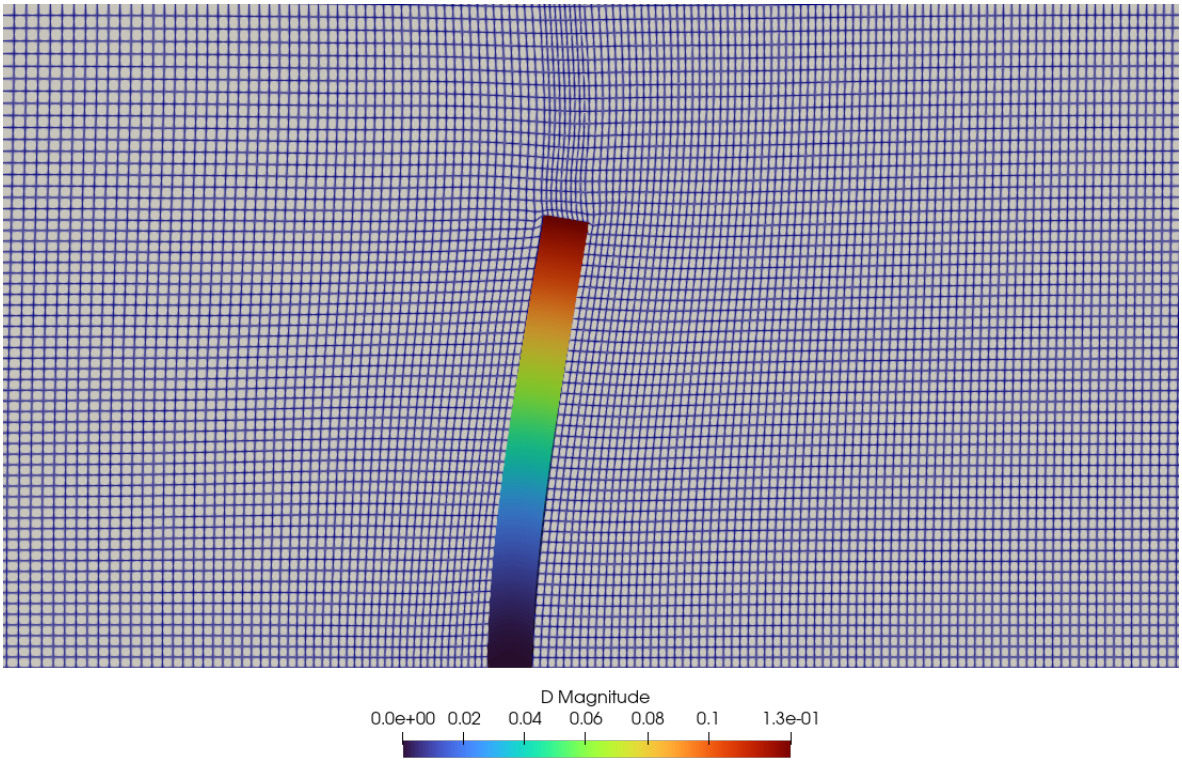

Figure 7: Mesh Morphing

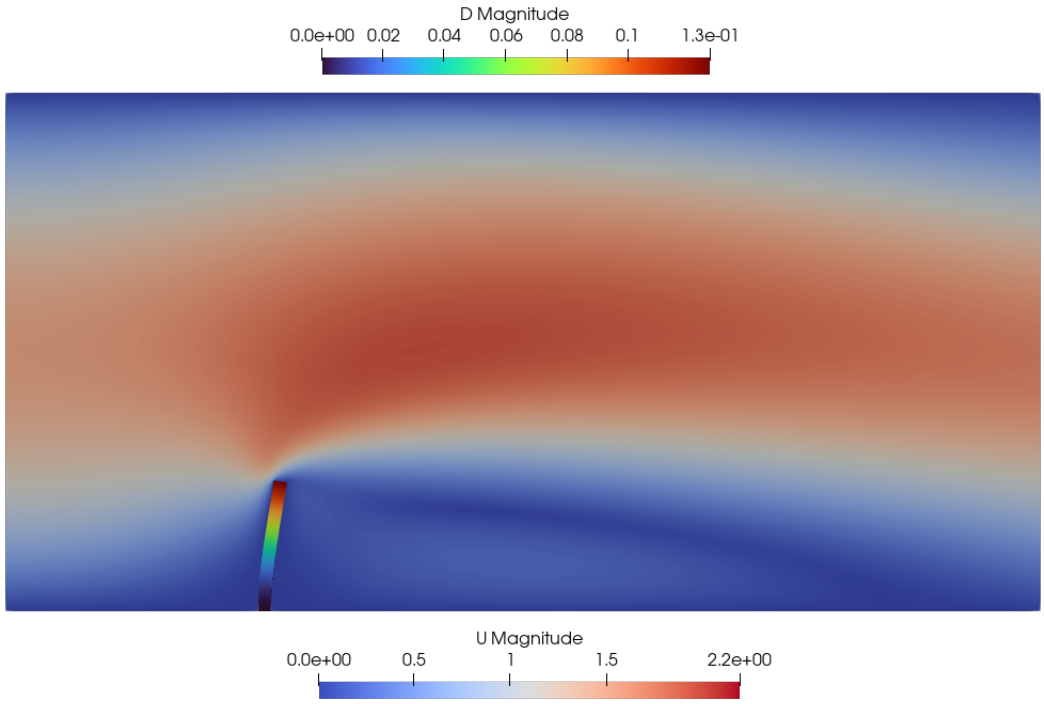

Figure 8: Displacement and Velocity Contours

4 Conclusions

In this study, the FSI between the flexible perpendicular flap and laminar incompressible flow has been done using the solids4foam solver. The density ratio between solid and fluid has been used as 10 with the flow Reynolds number being 25. The FSI has been done using two different coupling algorithms i.e. AITKEN and IQNILS and compared with each other as well as with the results obtained from the other solvers. To get the steady values of drag coefficient and displacement, 1e-6 is used as tolerance for the FSI loop associated with each time-step. The tolerance values higher than 1e-6 result in the oscillation in the values of drag coefficient and displacement.

CASE 2: HronTurek Case

5 Governing Equations and Models

5.1 Problem definition

This study focuses on the Fluid-Structure Interaction (FSI) in between the elastic plate and incompressible laminar flow. The geometry contains a rectangular horizontal channel as well as a rigid cylinder, with an elastic bar connected just behind the cylinder. This problem is based on the popular CFD benchmark in [4], commonly denoted to as the Hron-Turek Case. The FSI condition leads

to self-induced oscillations of the structure, mainly the elastic bar.

5.2 Governing equations

Fluid, solid, and the interface between them are governed by three sets of equations.

5.2.1 Fluid

The fluid is assumed as Newtonian and incompressible, with its state identified by the velocity and pressure field, denoted as v^f and p^f. The governing equations are:

$$\rho^f \frac{\partial v^f}{\partial t} + \rho^f \left(\nabla v^f\right) v^f = div\ \sigma^f \tag{9}$$

$$div\ \mathbf{v^f} = 0 \tag{10}$$

The solid material constitutive equation is

$$\boldsymbol{\sigma}^{\mathbf{f}} = -p^f \boldsymbol{I} + \rho^f \nu^f \left(\nabla \boldsymbol{v}^{\mathbf{f}} + \nabla \boldsymbol{v}^{\mathbf{f}\ T}\right) \tag{11}$$

5.2.2 Solid

The structure is supposed to be elastic and compressible, with its configuration represented by the displacement $u^s$and the velocity field given by $v^s = \frac{\partial u^s}{\partial t}$. The governing equations are:

$$\rho^s \frac{\partial^2 \boldsymbol{v}^{\mathbf{s}}}{\partial t^2} + \rho^s \left(\nabla \boldsymbol{v}^{\mathbf{s}}\right) \boldsymbol{v}^{\mathbf{s}} = div\left(\boldsymbol{\sigma}^{\mathbf{s}}\right) + \rho^s \boldsymbol{g} \tag{12}$$

The material is represented by the Cauchy stress tensor (σ^s) denoted by the following constitutive law for St. Venant-Kirchhoff materials:

$$\boldsymbol{E} = \frac{1}{2}\left(\boldsymbol{F}^{\mathbf{T}}\boldsymbol{F} - \boldsymbol{I}\right) \tag{13}$$

$$\boldsymbol{\sigma}^{\mathbf{s}} = \frac{1}{J}\boldsymbol{F}\left(\lambda^s\left(tr\ \boldsymbol{E}\right)\boldsymbol{I} + 2\mu^s \boldsymbol{E}\right)\ \boldsymbol{F}^T \tag{14}$$

5.2.3 Fluid-Solid Interface

The boundary conditions (BC's) at the fluid-solid interface are assumed to be:

$$\mathbf{v}_{\mathbf{f}}^{[\mathbf{i}]} = \mathbf{v}_{\mathbf{s}}^{[\mathbf{i}]} \tag{15}$$

$$\boldsymbol{u}_{\mathbf{fluid}}^{[\mathbf{i}]} = \mathbf{u}_{\mathbf{solid}}^{[\mathbf{i}]} \tag{16}$$

$$\boldsymbol{n}^{[\mathbf{i}]} \cdot \sigma_{\mathbf{fluid}}^{[\mathbf{i}]} = \mathbf{n}^{[\mathbf{i}]} \cdot \sigma_{\mathbf{solid}}{}^{[\mathbf{i}]} \tag{17}$$

where n is the unit vector perpendicular to the fluid-solid interface. This shows a no-slip condition for the fluid flow and make sure that the forces at the interface are in equilibrium.

5.3 Geometry and Mesh

The geometry contains a horizontal channel which is 0.41 m high and 2.5 m in length. A flexible flap, which is 0.02 m in width and 0.35 m in length, is connected just behind a rigid cylinder with the radius of 0.05 m. The center of the cylinder, which is point C, is located at (0.2, 0.2) m, with the origin situated at the bottom corner at left of the channel. The coordinate points are A(t), that is fixed to the structure at A(0) = (0.6, 0.2) m, and point B = (0.15, 0.2) m, representing the leading edge (LE) of the rigid cylinder which is facing the flow. The setup is maintained intentionally asymmetric to be free from dependence on computational precision for the formation of any associated potential oscillations. The geometry is illustrated in Figure 9.

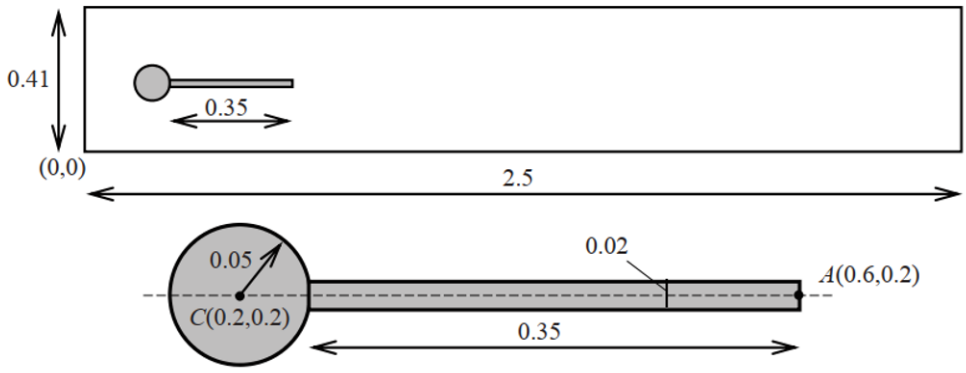

Figure 9: Computational Domain showing HronTurek Case

Meshing is done using Gmesh, an opensource meshing tool. In the FSI problem, while using the partitioned approach, the fluid domain and solid should be meshed separately since they are solved using different equations. The fluid domain is divided into eighteen different blocks and simple grading is used to create structured mesh near the rigid cylinder and elastic bar as shown in Figure 10. Similarly, a solid domain is meshed considering it as a single block as shown in Figure 11. Only hexahedral cells are used during the meshing of both fluid and solid domains.

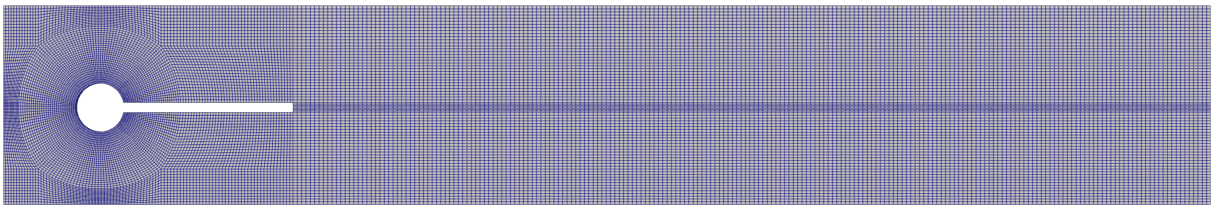

Figure 10: Mesh showing Fluid Domain

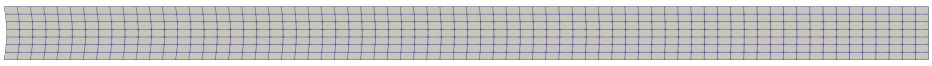

Figure 11: Mesh showing Solid Domain

5.4 Solver setup

The solver setup can be breakdown into three different parts: Fluid Setup, Solid Setup, and Coupling Setup

5.4.1 Fluid Setup

5.4.1.1 Initial and Boundary Conditions

The velocity of the fluid at the inlet varies parabolically with the width of the flap as given by the equation 18. There are actually 3 variants of this problem FSI1, FSI2 and FSI3 where FSI1 has steady state solution and other two results in periodic solutions. Only FSI 2 and FSI3 is analyzed with reference to the benchmark paper.

$$v^f(0,\ y)\ = 1.5\ \overline{U}\frac{4.0}{0.1681}y\ (0.41 - y)\ \ m/s \tag{18}$$

The Boundary Conditions applied at all patches are given in the Table 8 and 9:

Patch	Velocity	Pressure
inlet	transitionalParabolicVelocity	zeroGradient
outlet	zeroGradient	fixedValue
plate	newMovingWallVelocity	zeroGradient
cylinder	fixedValue	zeroGradient
bottom	fixedValue	zeroGradient
top	fixedValue	zeroGradient
frontAndBack	empty	empty

Table 8: Boundary Conditions for fluid domain

Patch	Point Displacement
plate	solidTraction
plateFix	fixedDisplacement
frontAndBack	empty

Table 9: Boundary Conditions for solid domain

5.4.1.2 Fluid Properties

The fluid's density is set at 1000 kg/m^3. A kinematic viscosity of 1e-3 m^2/s is used for both FSI2 and FSI3. The mean inlet velocity is 1 m/s for FSI2 and 2 m/s and FSI3 respectively. The flow is supposed to be in the laminar regime.

5.4.1.3 Dynamic Mesh Treatment

A mesh morphing approach is used in Solids4Foam to update the mesh regularly as the solid deflects and changes the fluid mesh. VelocityLaplacian Solver is used to handle the mesh motion within which the diffusivity quadratic inverseDistance method is selected.

5.4.1.4 Finite Volume Schemes

Operation and their Schemes are tabulated in Table 10.

Operation	Scheme
Time Derivative	Backward
Gradient	leastSquares

Divergence	default none;
	div(phi,U) Gauss upwind;
	div((nuEff*dev2(T(grad(U))))) Gauss linear;
	div((nuEff*dev(T(grad(U))))) Gauss linear;

Laplacian	Gauss linear corrected
Surface Normal Gradient	corrected
Interpolation	linear

Table 10: Finite Volume Schemes

5.4.1.5 Solution Method and Control

A GAMG solver with GaussSeidel smoother is used for pressure and cell displacemwnt. PBiCG with a DILU preconditioner is used for the velocity. The tolerance for the pressure, velocity and cell displacement is used as 1e-6.

5.4.2 Solid Setup

5.4.2.1 Boundary Conditions

Left end of the elastic bar is connected rigidly just behind the fixed cylinder and the other end is set free to deflection. It acts like a cantilever beam. The bar is not allowed to deflect in the z direction. When the fluid imparts pressure and viscous force to the bar then the bar deflects and starts oscillating when the flow becomes fully developed after two seconds.

5.4.2.2 Material Properties

The density of elastic bar is 10,000 kg/m3 and 1000 kg/m3 for FSI2 and FSI3 case respectively. The material properties of the elastic bar i.e. solid for both FSI2 and FSI3 are tabulated below in Table 11.

Properties	FSI2	FSI3
Density (kg/m^3)	10,000	1000
Young's Modulus (MPa)	1.4	5.6
Poisson's ratio	0.4	0.4

Table 11: Solid Properties for FSI2 and FSI3

5.4.2.3 Control

The time step of 1e−3 s is used.

5.4.3 Coupling Setup

Within the partitioned approach of two-way FSI, there can be two further different approaches: weak coupling and strong coupling. Weak coupling is also known as explicit coupling, and strong coupling is also known as implicit coupling. In implicit coupling, multiple iterations are done within a single coupling timestep to satisfy the dynamic and kinematic coupling conditions. In explicit coupling, only a single iteration is done without regard for dynamic and kinematic coupling conditions. In FSI cases like this, where the deflection is large, implicit coupling is a better approach as the accumulated error becomes too significant in explicit coupling. IQNILS is used as the coupling algorithm for the fluid solid interface. Value of 1e-6 is used as the tolerance for fluid solid interaction loop associated with each time step. And the maximum number of outer fluid solid interaction loop correctors is used as 30 associated with each time step. The relaxation factor is kept to 0.05 and the coupling is enabled after two second when the flow becomes fully developed.

6 Results and Discussions

6.1 Convergence Tests

6.1.1 Grid Size Convergence Test

Three different meshes are made using Gmesh for the Grid Convergence Test. It is done to make sure the results are not dependent of the cell size. A mesh refinement factor of two is used to create the coarse, medium, and fine mesh. This is done for the solid and fluid domains separately. The number of cells for all three coarse, medium, and fine mesh is tabulated in the Table 12 for fluid and solid separately.

Richardson extrapolation is done using the methodology mentioned in reference [5] to obtain the drag force when the cell size tends to zero. Ideally, this means an infinite number of cells in the fluid and solid domain. Then the relative percentage error is calculated for the drag coefficient values obtained for all three meshes by comparing with the Richardson extrapolated value which is shown in Table 13. By setting the criteria to be 1.5 % error and computational time, the medium mesh is chosen as the best one.

Mesh	Fluid Domain	Solid
Fine	12063	205
Medium	5787	102
Coarse	2788	48

Table 12: Number of cells for different meshes

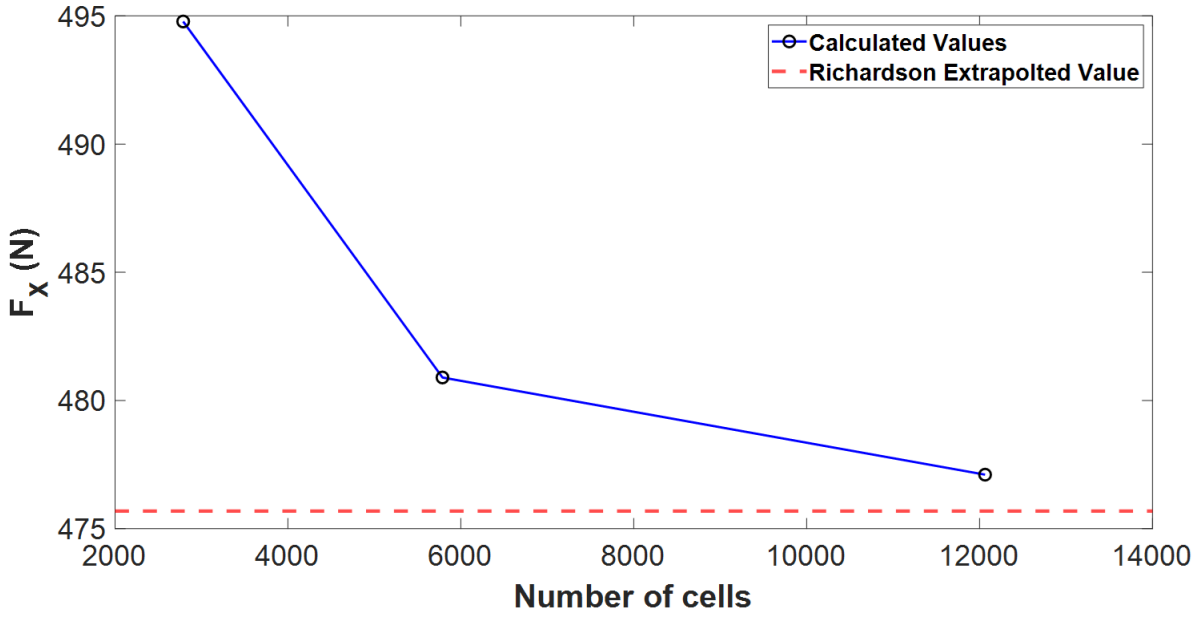

Figure 12: Grid Convergence Study considering F_x

Mesh	Force (F_x)	Relative Error (%)
Coarse	494.782	4.01
Medium	480.897	1.09
Fine	477.107	0.29

Table 13: Comparison with richardson extrapolated value

6.2 Validation

The converged values of forces and displacement in x and y direction for both FSI2 and FSI3 case are compared with benchmark values as tabulated in Table 14 and 15. The format of the data is mean ± amplitude[frequency].

FSI2	Benchmark	solids4Foam
$F_x(N)$	208.83 ± 73.75[3.8]	231.8215 ± 111.2485[4.44]
$F_y(N)$	0.88 ± 234.2[2.0]	1.1815 ± 352.2195[2.2676]
$D_x(mm)$	−14.58 ± 12.44[3.8]	-16.3165 ± 15.2522[4.44]
$D_y(mm)$	1.23 ± 80.6[2.0]	0.8832 ± 78.9590[2.2676]

Table 14: Comparison of FSI2 data with Benchmark

FSI3	Benchmark	solids4Foam
$F_x(N)$	457.3 ± 22.66[10.9]	480.897 ± 36.625[12.1951]
$F_y(N)$	2.22 ± 149.78[5.3]	0.999 ± 403.434[6.0241]
$D_x(mm)$	−2.69 ± 2.53[10.9]	-1.5903 ± 1.4607[12.1951]
$D_y(mm)$	1.48 ± 34.38[5.3]	1.7562 ± 25.0993[6.0241]

Table 15: Comparison of FSI3 data with Benchmark

6.3 Results

Maximum and minimum value of forces and disacement are employed for calculating the mean value and the amplitude of forces and dispacement which varies over time and when the solution becomes periodic which is 4 seconds for FSI 3 case. Amplitude as well as frequency of force and disaplacemt were calculated within the accuracy of 5% in comparison with the benchmark solutions. However, the mean value of drag force were calculated with error of 40% which is due to the problems associated with the calculation of mean value when its value is close to 0 as provided in [1]. X and Y displacement are plotted against time as shown in Figure 13 and 14. Similarly, the lift and drag forces are plotted against time as shown in Figure 15.

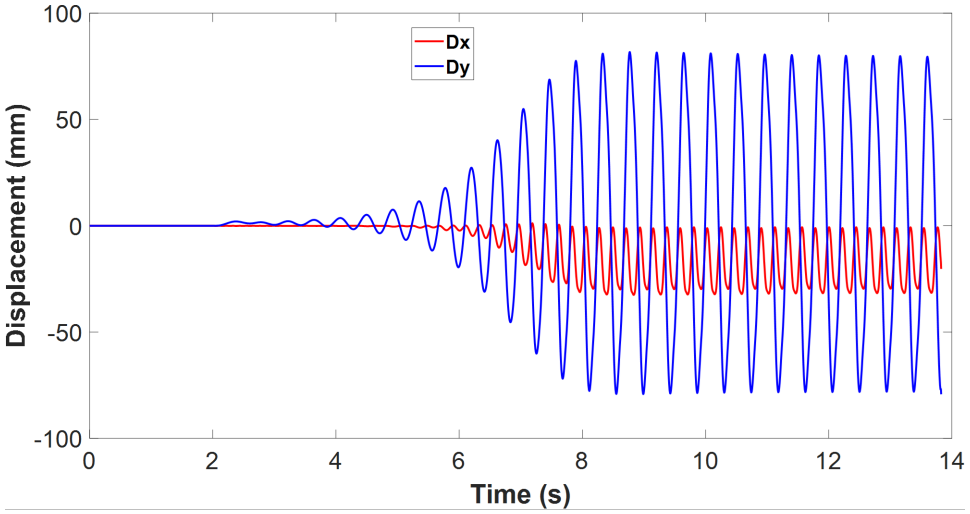

Figure 13: Displacement plot for FSI2

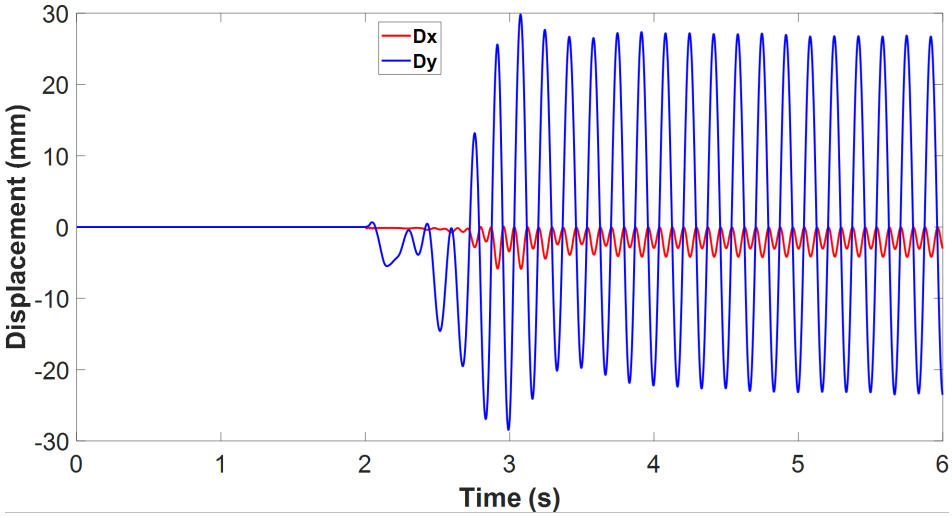

Figure 14: Displacement plot for FSI3

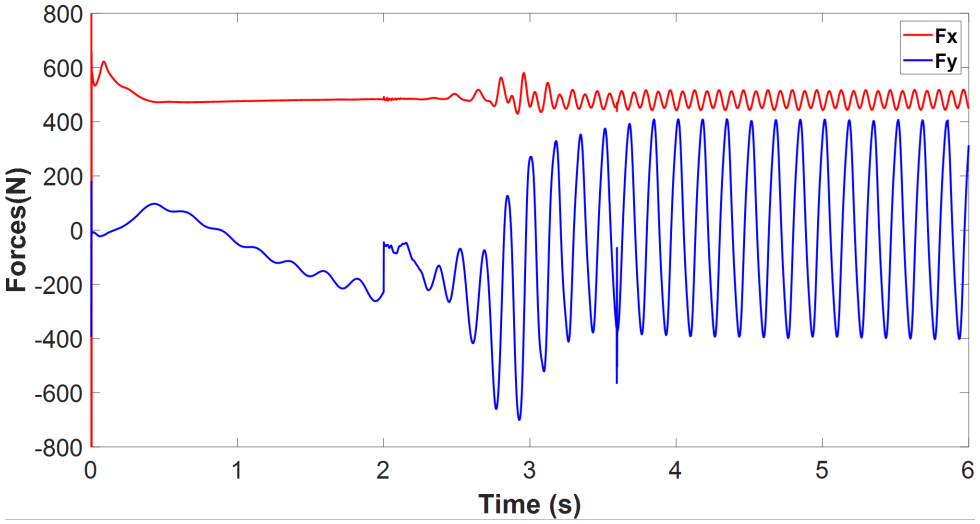

Figure 15: Force plot for FSI3

In Figure 17, displacement contours for the elastic bar and velocity contours in the fluid domain are shown simultaneously. It shows the position of the bar when the bar is oscillating after the flow becomes fully developed. Similarly, mesh motion of fluid domain due to elastic bar deflection is shown in Figure 16.

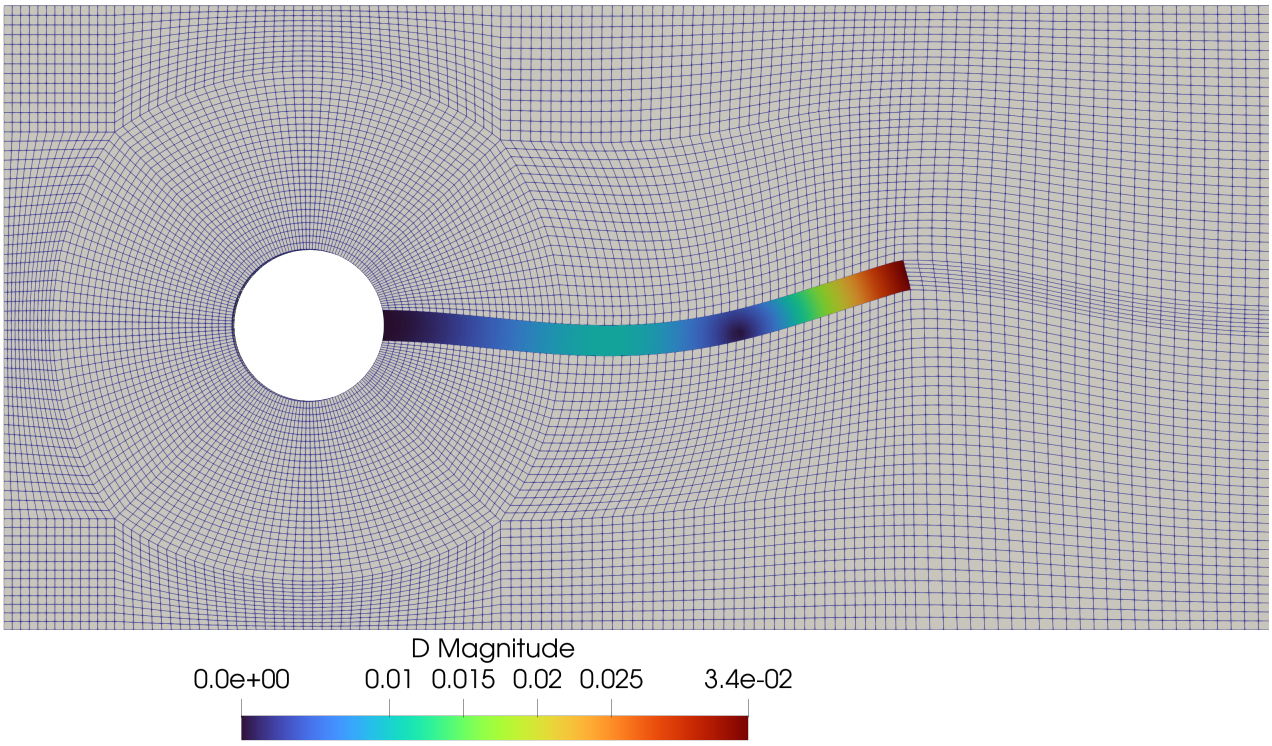

Figure 16: Mesh Motion due to bar oscillation

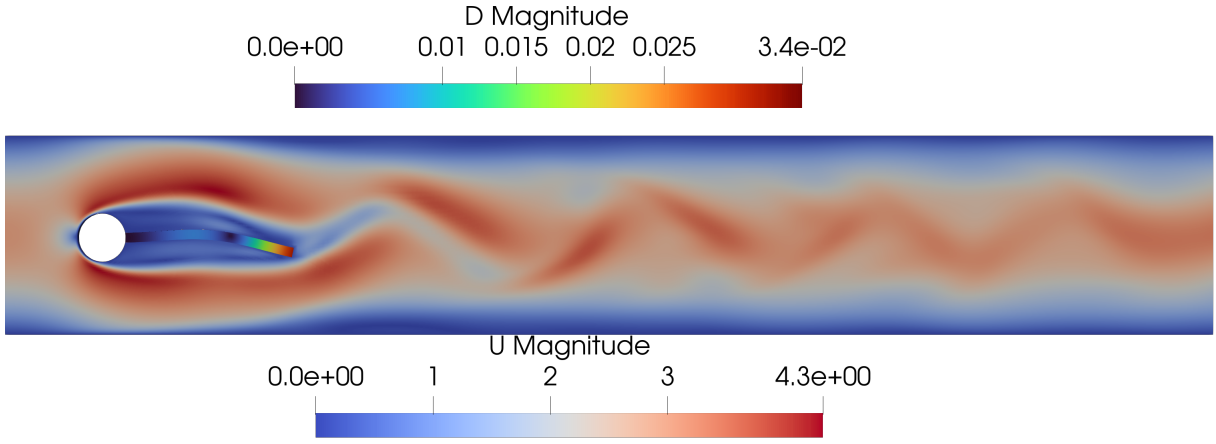

Figure 17: Contours when elastic bar is in deflected position

7 Conclusions

In this study, the FSI between the flexible elastic bar and laminar incompressible flow has been done using the solids4foam solver taking reference as the benchmark paper. Two different cases of HronTurek Problem are analyzed i.e. FSI2 and FSI3 cases with different properties of solid and

fluid. To get the steady values of drag force and displacement, simulation is run for 6 sec and 10 sec for FSI2 and FSI3 case respectively.

8 Acknowledgement

First and foremost, I'd want to express my profound appreciation to Dr. Chandan Bose, my supervisor, whose excellent insights and direction from the project's creation to completion were critical to its success and provided me with an invaluable learning experience. This endeavor would not have been feasible without him. I'd also want to thank Mr. Harish Jayaraj, my mentor for his important technical assistance. Last but not least, I'd like to thank Mrs. Payel Mukherjee, the FOSSEE team, and IIT Bombay for giving the opportunity, resources, and support necessary for the project's success.

References

[1] P. Cardiff, "solids4foam," 2020, accessed on 4-30-2024. [Online]. Available: http://www.solids4foam.com

[2] Philip Cardiff, "Training: Solid mechanics and fluid-solid interaction using the solids4foam toolbox," 06 2020.

[3] Z. Tuković, A. Karač, P. Cardiff, H. Jasak, and A. Ivanković, "Openfoam finite volume solver for fluid-solid interaction," *Transactions of FAMENA*, vol. 42, no. 3, pp. 1–31, 2018. [Online]. Available: https://hrcak.srce.hr/206941

[4] S. Turek and J. Hron, "Proposal for numerical benchmarking of fluid-structure interaction between an elastic object and laminar incompressible flow," in *Fluid-Structure Interaction*, H.-J. Bungartz and M. Schäfer, Eds. Berlin, Heidelberg: Springer Berlin Heidelberg, 2006, pp. 371–385.

[5] P. J. Roache, "QUANTIFICATION OF UNCERTAINTY IN COMPUTATIONAL FLUID DYNAMICS," *Annual Review of Fluid Mechanics*, vol. 29, no. 1, pp. 123–160, Jan. 1997. [Online]. Available: https://www.annualreviews.org/doi/10.1146/annurev.fluid.29.1.123